7th International Conference
on
Wind Turbine Noise
Rotterdam - 2nd to -5th May 2017

An Experimental Parametric Study of Airfoil Trailing Edge Serrations

T. Carolus **University of Siegen , 57068 Siegen, Germany**
E-Mail: **thomas.carolus@uni-siegen.de**

F. Manegar **University of Siegen, 57068 Siegen, Germany**
E-Mail: **farhan.manegar@uni-siegen.de**

E. Thouant **École Centrale de Lyon, Lyon, France**
E-Mail: **elodie.thouant@gmail.com**

K. Volkmer **University of Siegen , 57068 Siegen, Germany**
E-Mail: **kevin.volkmer@uni-siegen.de**

I. Schmich-Yamane **Électricité de France, Grenoble, France**
E-Mail: **isabelle.schmich-yamane@edf.fr**

ABSTRACT

Self-noise of an airfoil arises due to different mechanisms. In applications such as wind turbines the turbulent boundary layer interacting with the trailing edge is thought to be the dominant mechanism. In this study, a parametric study of add-on sawtooth type trailing edge serrations is carried out for trailing edge noise reduction. The main parameters which are known to control the performance of this trailing edge serrations type are the height and width of the serration teeth (i.e., amplitude and wavelength, respectively). Several parameters have been investigated experimentally in an aero-acoustic wind tunnel at the University of Siegen on a Somers S834 airfoil section. These parameters include the two main parameters mentioned above as well as orientation, thickness and the side on the airfoil, where serrations are attached. The experimental results show a maximum noise reduction for thin, long and narrow serration teeth, attached on the pressure side and oriented along the wake of the airfoil.

1. INTRODUCTION

Wind energy is a renewable source of energy and wind turbines convert energy without causing substantial adverse effects to the environment. However, the wide spread of wind turbines near densely populated regions is restricted mainly due to the emitted noise. Studies conducted to identify the noise sources from wind turbines have revealed that the dominant noise source is the flow induced trailing edge noise (TEN) [1]. An airfoil immerged in a flow emits TEN when the turbulent structures within the turbulent boundary layer (TBL) convect past the trailing edge (TE). These turbulent structures are scattered and radiated into the free field because of the edge discontinuity. TEN is broadband in nature [1].

Noise reduction techniques for TEN have been investigated since almost half a century now. They are classified into two types, active and passive. Some active techniques involve trailing edge blowing [2] and trailing edge suction [3]. Examples of passive techniques are the inclusion of porous trailing edges [4], serrations [5] and brushes [6] at the TE. Noise reduction techniques for wind turbines considering the practical constraints, converge towards trailing edge serrations (TES).

HOWE [7] contributed to the understanding of the effect of TES by deriving an analytical noise radiation model for low Mach number (Ma) flows to predict the noise reduction caused by sawtooth serrations on an infinite flat plate airfoil at zero angle of attack. More about HOWE's theory will be discussed in chapter 2. Many experimental works reported large deviations between the noise reduction experimentally achieved with TES and the noise reduction predicted with HOWE's model [5, 8-10]. LYU et al. [11] developed a new theoretical model and compared it with HOWE's model. In LUY's model the convection effects are incorporated in the convected wave equation, thereby making the model valid for all Ma numbers. In addition, by taking the effects of incident wall pressure gust into consideration the model tends to narrow down the deviation with the experiments. It was also enlightened that noise reduction is caused due to the destructive interference, i.e., out-of-phased scattered pressure in the vicinity of the TE.

JONES et al. [12] conducted direct numerical simulations (DNS) of the flow around a NACA-0012 airfoil with and without TES to understand the physical mechanism of TES. Two serration geometries were investigated, one with an amplitude $2h$ (see **Fig. 1**) equal to the boundary layer thickness δ at the TE (named as short) and another one with an amplitude of $2\,\delta$ (named as long), with wavelength λ being constant for both designs. Compared to the short TES the long TES provided higher noise reduction for all frequencies. The short TES provided less noise reduction and this only in a finite frequency range, above which the noise level increased. An interesting observation in this study was that the aerodynamic properties remained unchanged upstream of the TE for both cases, with and without TES. Hence the noise reduction is attributed to be caused due to the changes in scattering process and also due to the changes in the aerodynamic behavior in the direct vicinity of the serrations.

GRUBER [5] who did an extensive study of TES showed that the noise reduction is due to the reduction of phase speed at which the turbulence is convected near the sawtooth edges. In addition to that, a reduction of coherence of pressure measured along the sawtooth is also reported in the frequency band where noise reduction happens. OERLEMANS et al. [10] measured noise emission of a large scale wind turbine with one optimized blade, with serrations on another blade and the third blade remaining unaltered. His findings were that serrations resulted in a noise reduction of 2 – 3 dB; at higher frequencies a noise increase was observed,

which was explained to be due to misalignment of the serrations with the flow. VATHYLAKIS et al. [13] investigated the effect of flap angles on the noise reduction on a NACA65(12)-10 airfoil, where flap angles from -15° to + 15° in steps of 5° have been studied. The flap-up position (+5°), which is oriented towards the suction side, resulted in the best noise reduction, the flap-down position (-5°) was the worst configuration.

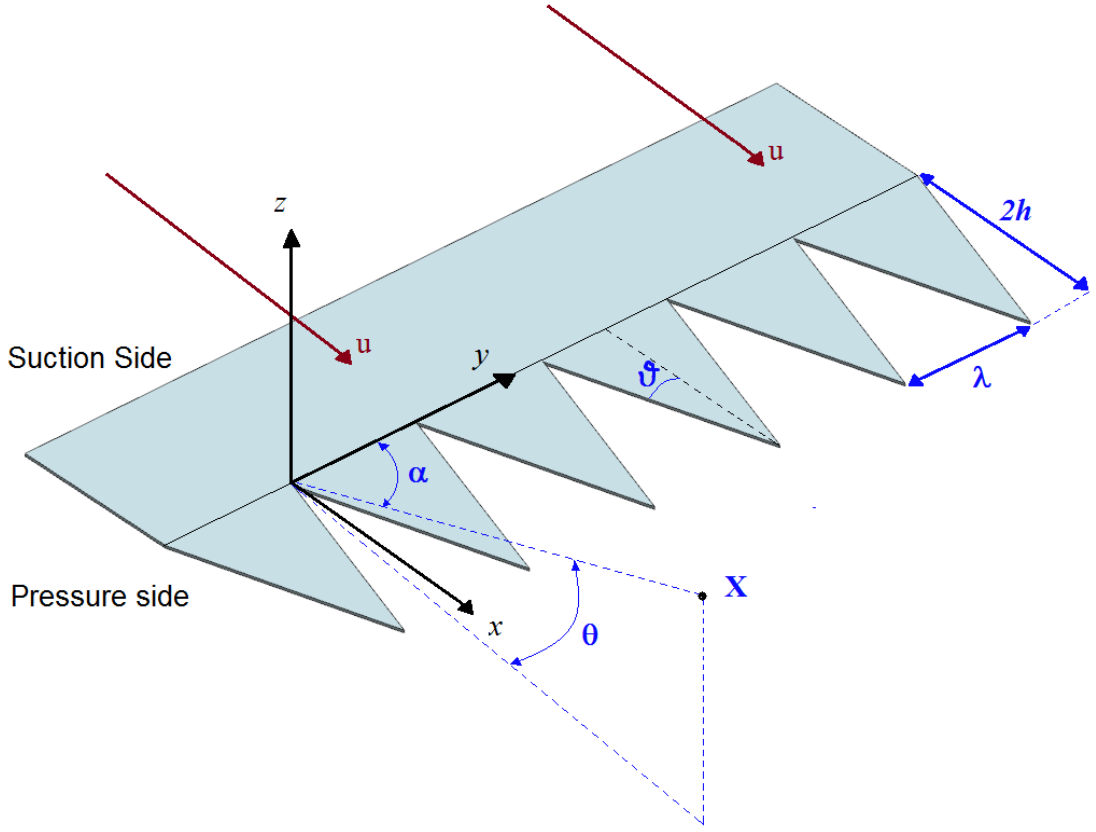

Fig. 1 Geometrical parameters of a serrated trailing edge and the coordinate system.

This paper presents a preliminary experimental model scale study on the acoustic effect of various parameters apart from the classical serration geometry "amplitude" and "wavelength", which could influence the noise reduction capability of TES. Additionally, a discussion on some findings of other researchers like deviation between experiment and HOWE's model, effects of flap angle and effects of serration amplitude.

2. HOWE's theory

The serrations which are investigated in this work are designed based on HOWE's theory leading to a specific design of TES. A brief description of his theory is presented in this section.

HOWE [7] derived an analytical model for predicting the noise from a flat plate at zero angle of attack with sawtooth serrations attached to TE. The sawtooth serrations have a spatial periodicity called as wavelength λ and a root-to-tip distance called as amplitude *2h* as shown in **Fig 1**. Green's function is used to calculate the pressure radiated to the observer's location. The use of modified Green's function in the case of serrated TE is argued by LYU et al. [11], who instead proposes to calculate scattered sound using the convected wave equation.

This is the reason why HOWE's model is valid only for low Ma numbers, because it neglects the effects of convection (the direct radiation to the far field due to the quadrupole sources in the boundary layer). HOWE also assumes that the properties of turbulence remain the same before and after the TE within the boundary layer, in other words, he assumes a frozen turbulence.

Using CHASE's [14] model for wavenumber frequency spectrum of the blocked wall pressure inside the turbulent boundary layer, the far-field sound power spectrum at the observer point at a distance |X| from TE is given as in eq. (1)

$$\frac{\Phi(\mathrm{X},\omega)}{\left(\rho\upsilon_*^2\right)^2\left(l/c_0\right)\left(\delta/|\mathrm{X}|\right)^2}=\left(\frac{C_m}{\pi}\right)\sin^2\left(\frac{\theta}{2}\right)\sin(\alpha)\Psi(\omega), \tag{1}$$

where ρ is the fluid density, l is the span, c_0 is the speed of sound, δ is the turbulent boundary layer thickness, θ and α are respectively polar and azimuthal observer angles, $\omega = 2\pi f$, where f is the frequency, skin friction coefficient $\upsilon_* \approx 0.03u$; $C_m \approx 0.1533$, $\varepsilon \approx 0.133$ are constants and the convection velocity is $U_c \approx 0.7u$. The non-dimensional edge noise spectrum is

$$\Psi(\omega)=\left(1+\frac{1}{2}\varepsilon\frac{\partial}{\partial\varepsilon}\right)f\left(\frac{\omega\delta}{U_c},\ \frac{h}{\lambda},\ \frac{h}{\delta};\ \varepsilon\right),$$

where

$$f\left(\frac{\omega\delta}{U_c},\ \frac{h}{\lambda},\ \frac{h}{\delta};\ \varepsilon\right)=\frac{1}{ab+\varepsilon^2}\left(1+\frac{64\left(h/\lambda\right)^3\left(\delta/h\right)\left(\cosh\left(c\sqrt{a+\varepsilon^2}\right)-\cos\left(2\omega h/U_c\right)\right)}{\left(\sqrt{a+\varepsilon^2}\right)\left(ab+\varepsilon^2\right)\sinh\left(c\sqrt{a+\varepsilon^2}\right)}\right)$$

$$a=\left(\omega\delta/U_c\right)^2,\ b=1+\left(4h/\lambda\right)^2,\ c=\lambda/2\delta,\ \varepsilon=1.33$$

The normalized spectra $10\log\left[\Psi(\omega)\right]$ (dB) for λ/h = 0.25, 1, 5 and h/δ = 1 and h/δ = 3, along with the spectrum for unserrated edge (not defined here, refer [7]) are plotted in **Fig 2**.

The important factors which control the noise reduction mechanism according to HOWE are as follows:

1) Noise reduction takes place when the non-dimensional frequency $\omega\delta/u$ is larger than 1.
2) The angle ϑ between mean flow and the local tangent to the wetted region should be less than 45º, i.e., the sharper the serrations, the higher the noise reduction.
3) Higher noise reductions occur when the dimensions of the serrations are of the order of the turbulent boundary layer thickness δ and more.

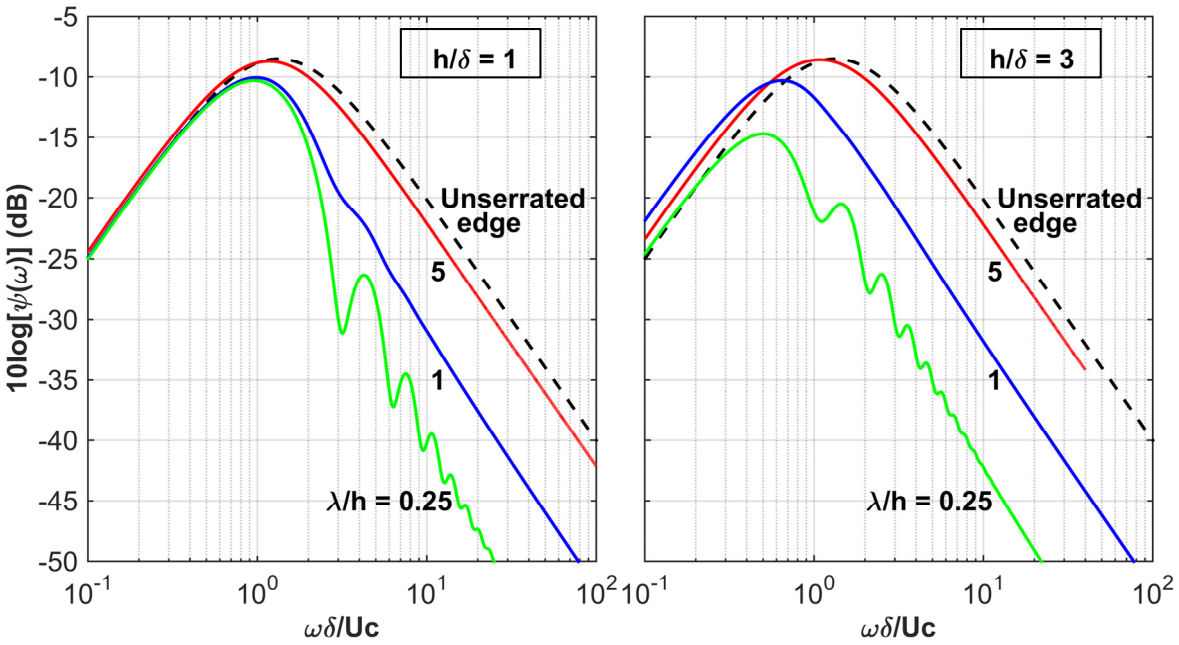

Fig. 2 HOWE's model: Normalized acoustic pressure frequency spectrum for unserrated and serrated edge as a function of λ/h and h/δ.

3. Experimental setup

3.1 Airfoil investigated and aero-acoustic wind tunnel

The experimental investigation was carried out with SOMERS S834 airfoil segment, with a chord length of 0.2 m and a span of 0.266 m in an aero-acoustic wind tunnel facility at the University of Siegen shown in **Fig. 3.** For an airfoil in a confined jet, it is essential to apply a correction factor for the angle of attack (AOA) as stated by BROOKS et al. [15]. This is due to the fact that the lifts produced by an airfoil in a free stream and in a confined jet are not the same, as the finiteness of the jet leads to significant flow deflection. The effective AOA for this study has been chosen such that an infinitely long span of the airfoil has maximum glide ratio. It has been calculated using XFOIL. The result is 4.7°. On applying the correction factor, the geometric AOA is obtained as 12.7°.

The airfoil segment is mounted between the side plates at the end of the contracting nozzle. A centrifugal fan is used to create the desired flow rate and the air is passed through a series of screens, honeycomb and silencers. The aero-acoustic wind tunnel provides a maximum flow velocity u = 25.55 m/s. The chord based Reynolds number (Re) is 350000. In order to replicate or mimic the real conditions in a large wind turbine, a ten times higher Re has to be achieved. Hence the airfoil is tripped at the natural transition position that occur at $3.5 \cdot 10^6$. The tripping positions are calculated using XFOIL and a zig zag trip is applied along the complete span at 34 mm from the leading edge (LE) on the suction side (SS) and 152 mm from the LE on the pressure side (PS).

3.2 Acoustic measurement

The wind tunnel exhausts in a semi-anechoic chamber which allows the acoustic measurements according to ISO 3745. The cut-off frequency of the chamber is 125 Hz. The dimensions of the semi-anechoic chamber are 4.5 m x 3.23 m x

2.9 m. The turbulence intensity of the jet is 0.2 % at a plane 0.01 m downstream the exit of the nozzle. The floor in the chamber is reflective and has an opening covered with grid, through which the flow recirculates. More details about the semi-anechoic chamber can be read in [16].

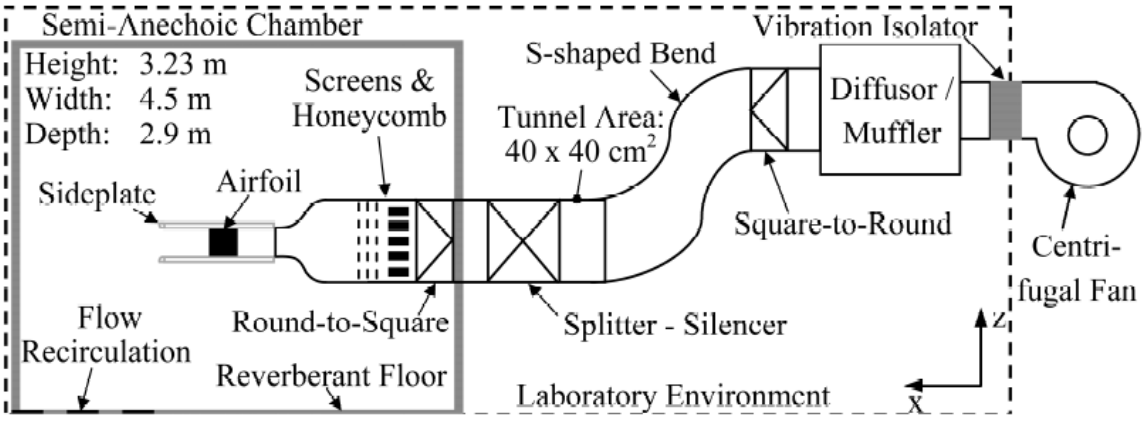

Fig. 3 Schematic diagram of aero-acoustic wind tunnel (not to scale)

Three microphones (1/2" Brüel & Kjaer TM, type 4190) are used to measure synchronously the noise being emitted from the airfoil. The microphones are covered with wind screens to avoid any flow induced pseudo sound and are located at a distance of 2.5 times chord (500 mm) from the TE as shown in **Fig 4**. All measurements are captured with a sampling rate of f_s = 51.2 kHz. The spectral analysis is based on the power spectral density S_{pp} obtained using the *pwelch* routine in Matlab™ Vers. R2014b (Δf_{ref} = 1 Hz, $p_0 = 2 \cdot 10^{-5}$ Pa). L_{Spp} is defined as shown in eq. (2)

$$L_{Spp}(f) = 10 \cdot \lg\left(\frac{S_{pp} \cdot \Delta f_{ref}}{p_0^2}\right) \quad [\mathrm{dB}] \tag{2}$$

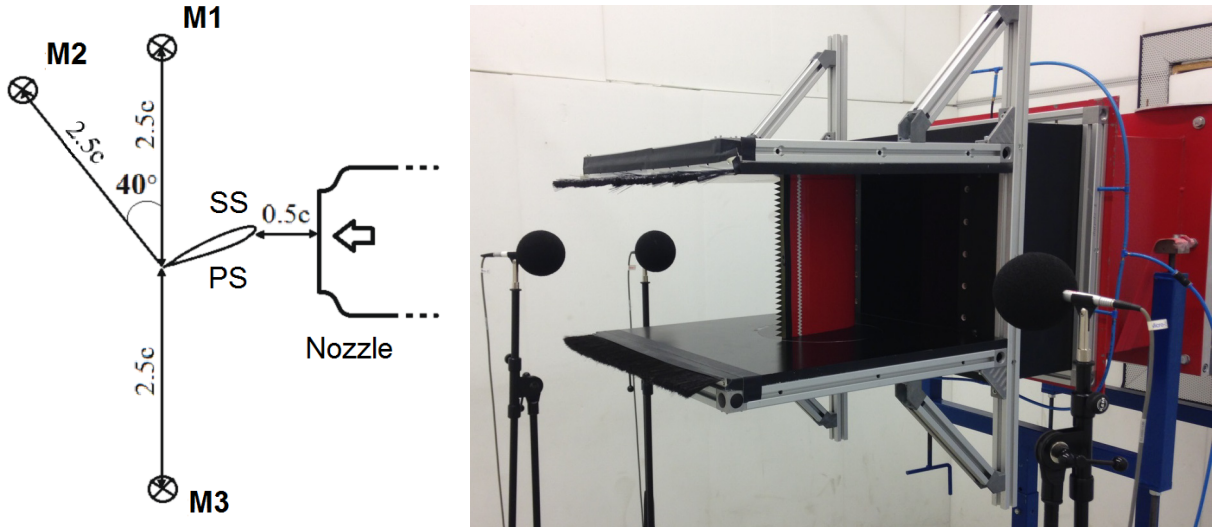

Fig. 4 Left: Schematic diagram of microphone locations, right: Microphones in semi anechoic chamber.

During TEN measurements the background noise due to the wind tunnel contaminates the acoustic signature of the airfoil Therefore, the measurements were

done once with the reference airfoil and once without, to estimate the influence of the background noise. The L_{spp} spectrum of all three microphones averaged is shown in **Fig 5**. It has to be noticed that the signal to noise ratio is bad in frequency ranges above 3000 Hz, i.e., the background noise is too high in these frequency to separate airfoil from background noise. Hence in this study, the investigations of TES will be only displayed in a frequency range from 200 Hz to 3000 Hz.

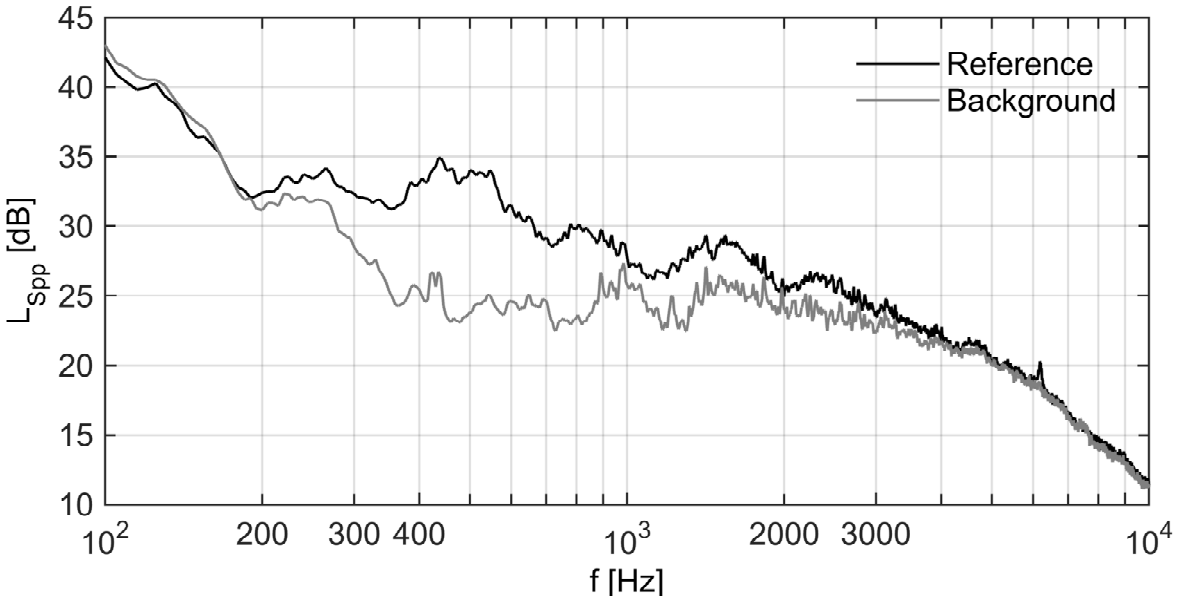

Fig. 5 L_{spp} of reference airfoil and background noise at microphone locations as shown in **Fig. 4** (average of 3 microphones).

3.3 Serrations investigated

As mentioned earlier, the serrations in this study are designed based on HOWE's theory and the following two parameters are defined to design the serration:

- The relative length h/δ, where h is half of serration's amplitude and δ is the boundary layer thickness at the TE, which is obtained from the experimental results of reference airfoil for the same flow characteristics conducted by GERHARD [17]. The here used value of δ is 9 mm.
- The relative wavelength λ/h, where λ being serration's wavelength.

To achieve noise reduction, the designed serrations must satisfy the following two conditions stated by HOWE:

- $1 < h/\delta | < 10$
- $\lambda/h < 4$ or $\vartheta < 45°$

Before the various designs were investigated, a parametric study of three following important parameters was carried out:

- Fixation side: The side on which serrations are glued.
- Orientation: The angle φ the serration makes with respect to the camber line of the airfoil. The serrations oriented towards the suction side (SS) have positive values of φ and the serrations oriented towards the pressure side (PS) have negative values of φ. The serration aligned to camber line has $\varphi = 0°$. Orientation angles between +15° and -15° in steps of -5° have been investigated.

- Relative thickness t/δ, where t is the thickness of the serration and δ is the boundary layer thickness: the values of t/δ = 0.56 %, 3.3 %, 5.6 % and 11 % have been investigated.

After evaluating the results from this parametric study, the following three sets of serrations incorporated with the best fixation side, orientation and relative thickness are investigated:

Set 1: λ/h = 0.25, 1.00 , 5.00 with h/δ = 1

Set 2: λ/h = 0.25, 1.00, 1.50, 2.00, 2.50, 5.00 with h/δ = 3

Set 3: h/δ = 1.00, 1.50, 2.00, 2.50, 3.00 with λ/h = 1

All the parameters are shown in the schematic diagram in **Fig. 6** (left). A photograph of the serrations of Set 2 is shown in the right side of **Fig 6**.

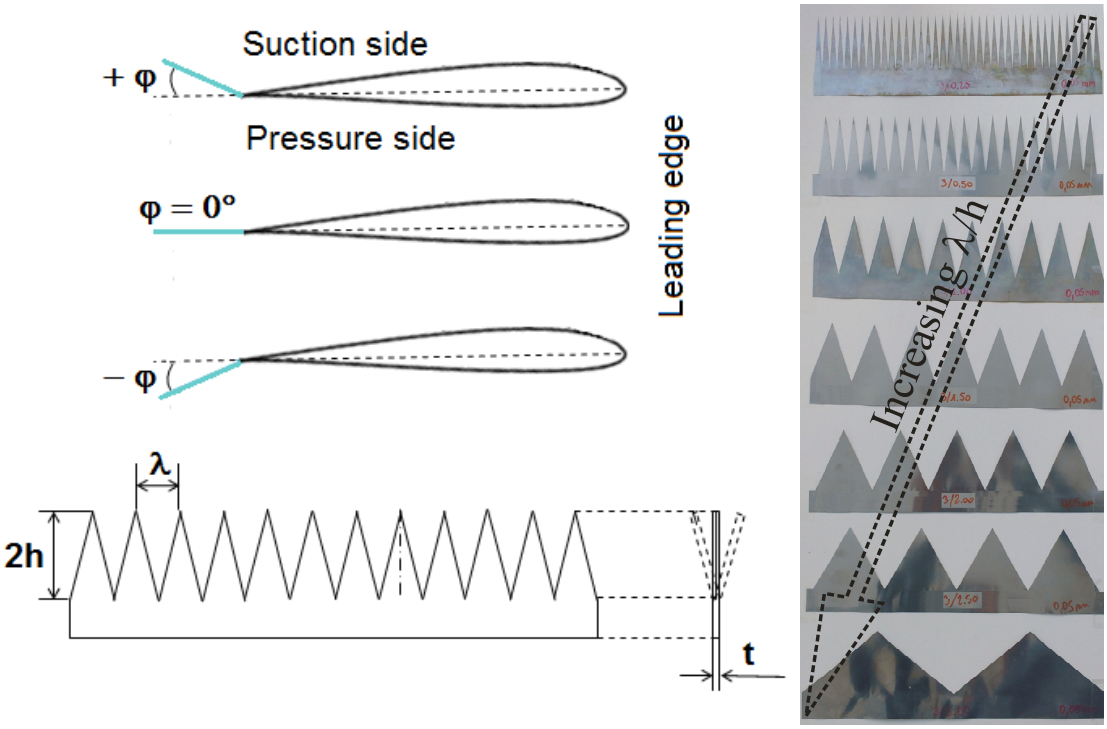

Fig. 6 Left: Schematic diagram of serration parameters, right: Serrations of Set 2.

4. Results

Three main parameters are analyzed one after the other. The best result in each analysis is kept for the next parameter's analysis.

4.1 Fixation side

For this investigation, a serration having h/δ = 1 and λ/h = 1 with a relative thickness t/δ = 0.67 % and the orientation angle φ = +5° is chosen. Measurements are carried out with this serration glued on the SS and PS respectively. It is to be noted that, when the serration is glued on the PS, the orientation angle is naturally φ = +5°, but when it is glued on the SS, the serration has to be oriented towards the SS to yield the same orientation angle φ = +5°(**Fig 7**).

The L_{SPP} spectra for both cases are plotted in **Fig. 8** along with the L_{SPP} spectrum for the reference case without TES. It is observed that the serration when glued on SS results in less noise reduction in comparison to the serration glued on PS. Hence for the following investigations, the serration is glued on the PS.

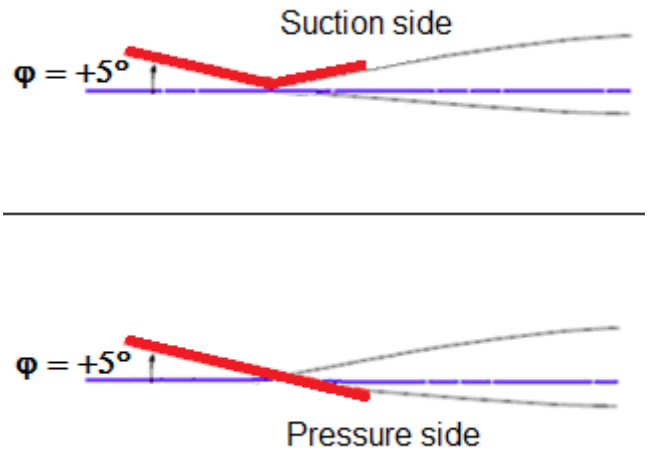

Fig. 7 Schematic diagram of different fixation sides of TES.

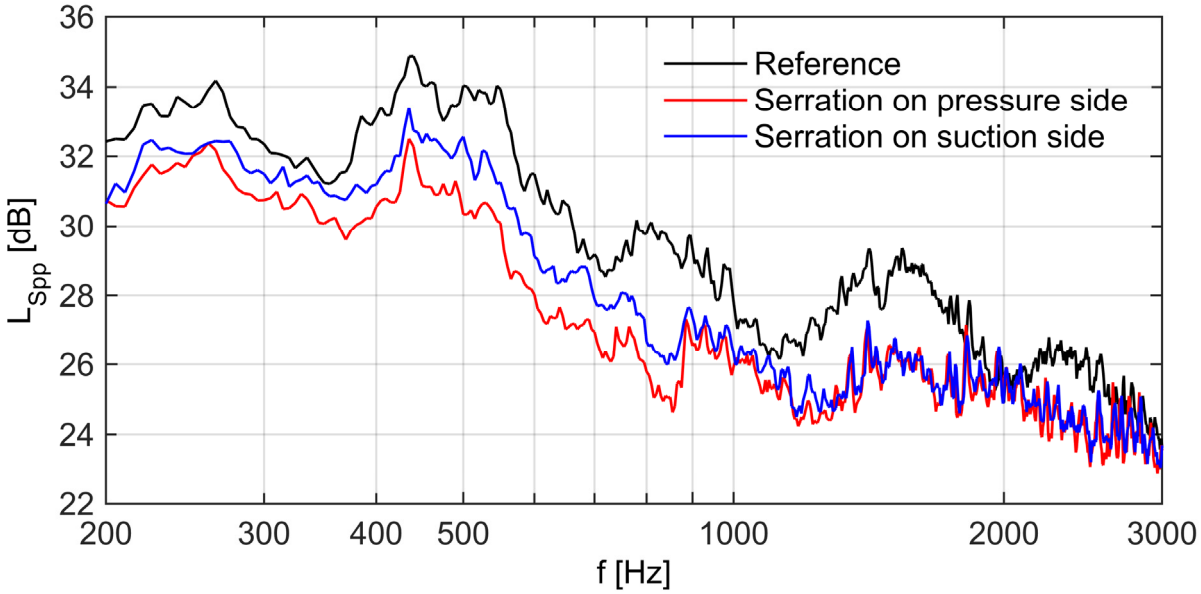

Fig. 8 Effect of fixation side of serrations.

4.2 Orientation

For this investigation, a serration having h/δ = 1 and λ/h = 1 with a relative thickness of t/δ = 3.3 % is chosen and glued on the PS. Measurements are carried out for orientation angles φ = +15° to -15° in steps of -5°. As mentioned earlier, the serrations orienting towards SS have positive values of φ and the serrations orienting towards PS have negative values of φ. The serration aligned to the camber line has an angle φ = 0°. The results are presented in three figures. First a comparison of φ = +15°, 0° and -15° is shown in **Fig 9a**. It is to be noted that the serration oriented towards SS (φ = +15°) brings a potential reduction only beyond 600 Hz. On the contrary, the serration oriented towards PS (φ = -15°) increases noise emission beyond 600 Hz. The serration aligned with camber line (φ = 0°) reduces the TEN almost in the entire frequency range displayed. In **Fig. 9b**, the comparison of φ = -10°, 0° and 10° is shown. The same tendency is observed here except for the fact that the frequency at which the change of behavior happens is shifted to 750 Hz, which was 600 Hz in the previous case.

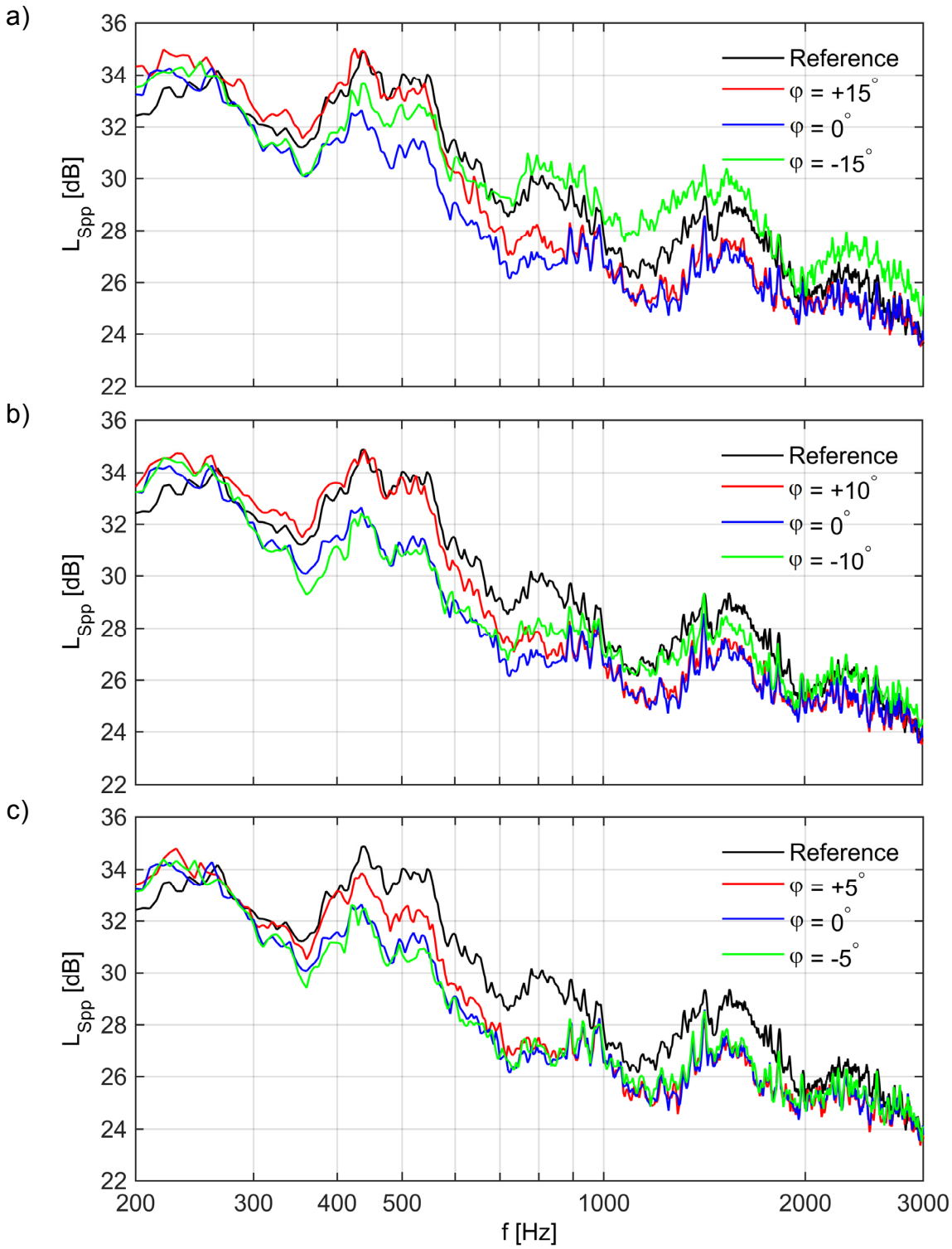

Fig. 9 Effect of orientation angle φ.

The serration aligned with the camber line (φ = 0°) seems to be still the best configuration. Finally the comparison of φ = -5°, 0° and +5° is shown in **Fig 9c**. Here it is observed that, all three orientation angle reduce the noise emission and the best noise reduction is provided by the serration with φ = -5°. This is contradicting with the results presented by VATHYLAKIS et al. [13]. However, for the next investigations, the orientation angle φ = +5° will be implemented, because to achieve φ = -5°, the serrations have to be bent manually towards the SS and the risks of misaligning some of the tooth is high, whereas with φ = +5° the serrations

need to be glued on the PS and requires no further bending.

4.3 Relative thickness

Another interesting parameter to be investigated is the relative thickness of the serration. For this investigation, a serration having h/δ = 1 and λ/h = 1 with the orientation angle φ = +5° is chosen and is glued on the PS. Four different relative thicknesses of serration were investigated, t/δ = 0.56 %, 3.3 %, 5.6 % and 11 %. The measurement results are shown in **Fig 10** for only three of them.

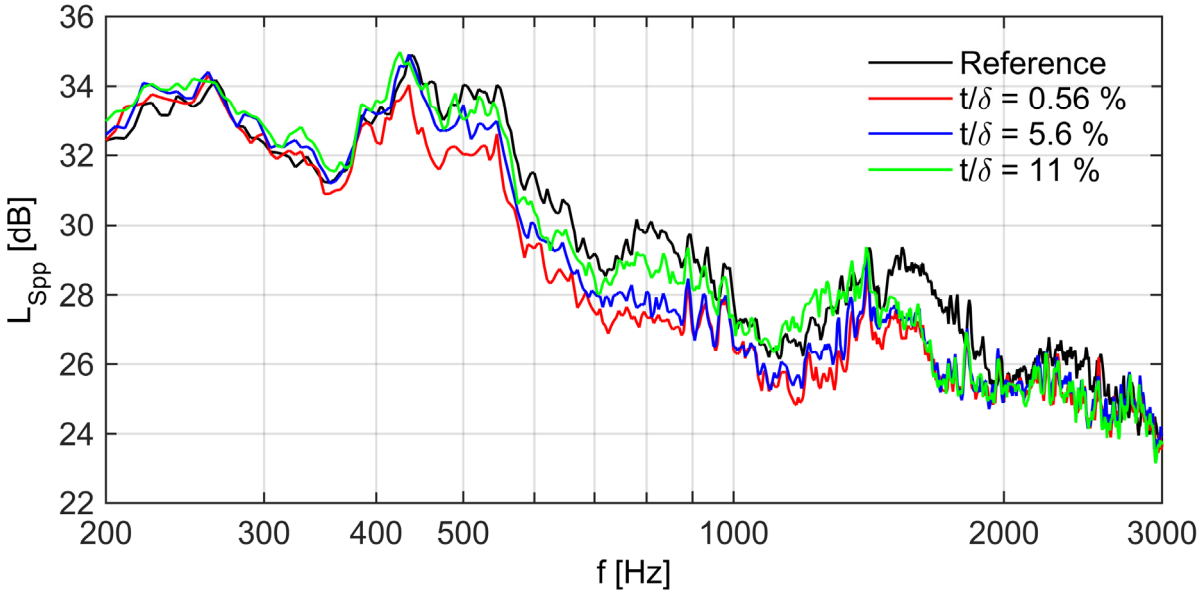

Fig. 10 Effect of relative thickness of serrations t/δ.

The results show that the variation of thickness does not have a big influence in noise reduction. However it is observed that the thinner the serrations are the higher is the noise reduction. For further investigation, the serration with t/δ = 0.56 % is chosen.

4.4 Serrations based on HOWE's theory

As already stated, all the serrations investigated in this section are glued on the PS with φ = +5° and t/δ = 0.56 %. At first an analysis is made between serrations which have a constant h/δ (1 and 3) but varying λ/h (0.25, 1, 5), i.e., Set 1 and Set 2. The measurement results are shown in **Fig 11.a** and **Fig 11.b**. The following two observations are made:

- The longer the serrations, the higher the noise reduction. This is in agreement with the observations in simulations by JONES et al. [12].
- According to HOWE, the sharper the serrations, the higher is the noise reduction. But in both cases presented below, the serration with λ/h = 0.25 has lesser noise reduction compared to λ/h = 1.

Another interesting comparison is presented in **Fig 11.c**, where the serrations are increased in amplitude from h/δ = 1 to 3 in steps of 1 and the wavelength is kept the same of half of amplitude in each case. A clear increase in noise reduction can be seen for the frequency range 300 Hz to 800 Hz, as the serrations become longer and broader.

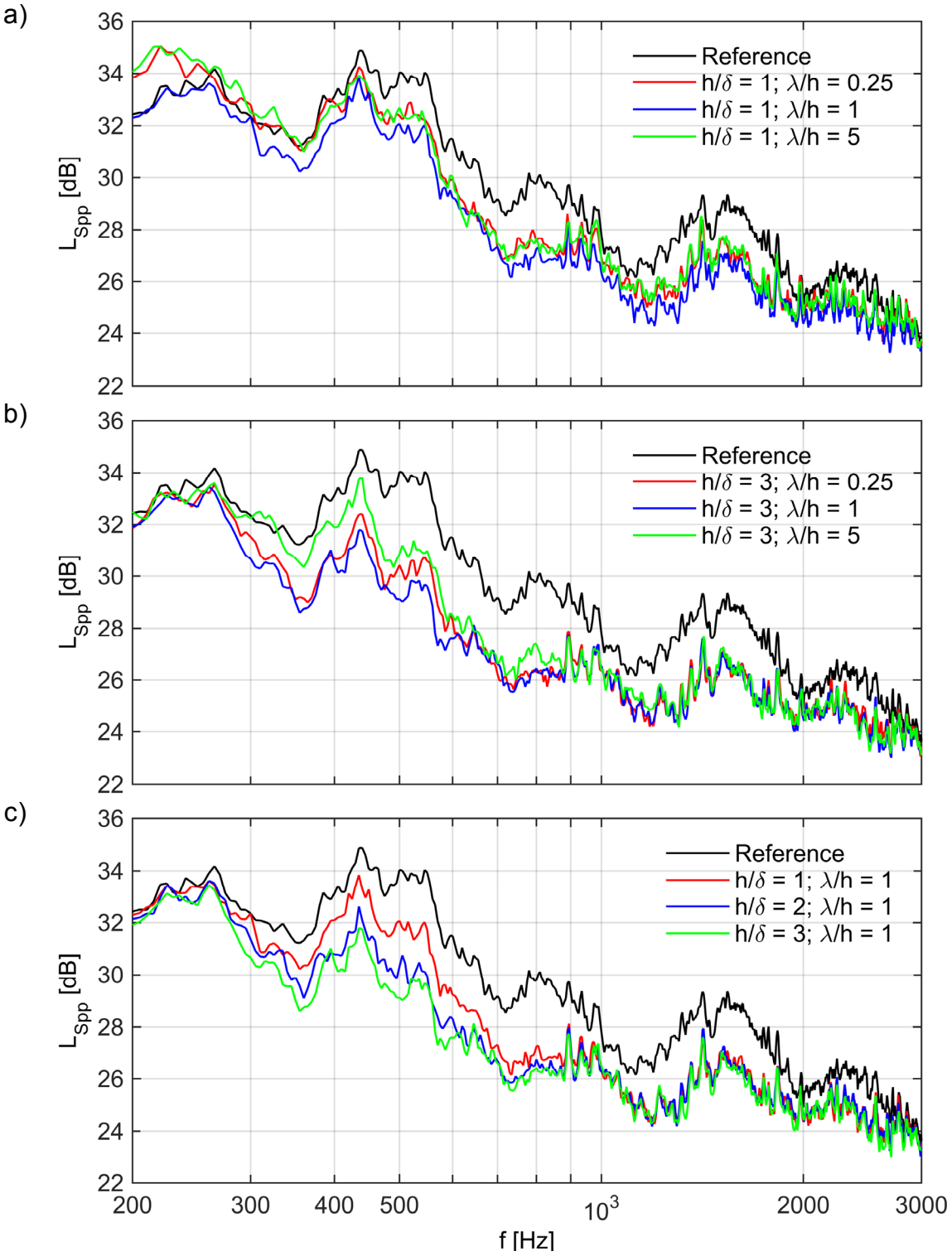

Fig. 11 Effect of "amplitude" and "wave length" of serrations; a) set 1, b) set 2, c) set 3.

The results of other investigated serrations are not shown here. The serration which brought about the least noise reduction was h/δ = 1 and λ/h = 0.25. The best serration is the one with h/δ = 3 and λ/h = 1. With this geometry a noise reduction of 3 dB was achieved in the frequency range from 300 Hz to 900 Hz with a maximum of 5 dB noise attenuation at the TE peak around 500 Hz. This finding corresponds to GRUBER's [5] who also reported that the serrations with h/δ > 2

yield the maximum noise reduction. However, the increase in noise beyond $f\delta/u > 1$, as reported by Gruber, was not observed here due to the insufficient signal-to-noise ratio.

5. Conclusion

In this study a variety of triangular type trailing edge serrations have been designed based on HOWE's theory and eventually investigated in model scale experiments. On top of the classical design parameters h/δ and λ/h, more technological parameters have been investigated. The outcome was that it is beneficial to glue the serration on the pressure side rather than the suction side and to keep the thickness at 0.05 mm (i.e., t/δ = 0.56 %). The best angle of orientation is φ = +5°, which means the serration is oriented towards the pressure side, aligning most probably with the wake, which has not been quantified in this study. The investigation of various serrations based on HOWE's theory showed that the serrations having h/δ = 3 and λ/h = 1 bring best results. Previous predictions that smaller values of λ/h result in better noise reduction could not be confirmed within this study.

ACKNOWLEDGEMENTS

The authors would like to thank Michel Roger (École Centrale de Lyon) and Marlene Sanjose (University of Sherbrooke) for their technical advice and also the workshop at University of Siegen for manufacturing the serrations. Part of this work has been funded by the Federal Ministry for Economic Affairs and Energy of Germany (BMWi) within the project RENEW (FKZ 0325838B).

REFERENCES

[1] OERLEMANS, S., SIJTSMA, P., MÉNDEZ LÓPEZ, B.M., 2007, "Location and quantification of noise sources on a wind turbine", *Journal of Sound and Vibration*, **299**: 869-883.

[2] GERHARD, T., ERBSLÖH, S., CAROLUS, T., 2014, "Reduction of airfoil trailing edge noise by trailing edge blowing", *Journal of Physics*, **524**: 012123.

[3] WOLF, A., LUTZ, T.H., WURZ, W., KRAMER, E., STALNOV, O., SEIFERT, A., 2015, "Trailing edge noise reduction of wind turbine blades by active flow control", *Wind Energy 18*, **909**.

[4] SARRADJ, E., GEYER, T., 2007, "Noise generation by porous airfoils", *28th AIAA Aeroacoustics Conference.* 2007-3719.

[5] GRUBER, M., 2012, "Airfoil noise reduction by edge treatments", *Ph. D. thesis.*

[6] HERR, M., 2013, "Trailing edge noise - Reduction concepts and scaling laws", *Ph. D. thesis.*

[7] HOWE, M.S., 1991, "Noise produced by a sawtooth trailing edge", *The Journal of the Acoustical Society of America*, **90**: 482-487.

[8] DASSEN, A.G.M., PARCHEN, R., BRUGGEMAN, J., HAGG, F., 1996, "Results of a wind tunnel study on the reduction of airfoil self-noise by the application of serrated blade trailing edges", *Proceeding of the European Union Wind Energy Conference and Exhibition*, pp. 800-803.

[9] PARCHEN, R., HOFFMANS, W., GORDNER, A., BRAUN, K., 1999, "Reduction of airfoil self-noise at low Mach number with a serrated trailing edge", *6th International*

Congress on Sound and Vibration, pp. 3433-3440.

[10] OERLEMANS, S., FISHER, M., MAEDER, T., KÖGLER, K., 2009, "Reduction of wind turbine noise using optimized airfoils and trailing-edge serrations", *AIAA Journal*, Vol. **47**, pp. 1470-1481.

[11] LYU, B., AZARPEYVAND, M., SINAYOKO, S., 2015, "A trailing-edge noise model for serrated edges", *21st AIAA/CEAS Aeroacoustics Conference*, pp. 1-24.

[12] JONES, L.E., SANDBERG, R.D., 2012, "Acoustic and hydrodynamic analysis of the flow around an aerofoil with trailing-edge serrations", *Journal of Fluid Mechanics*, Vol. **706**, pp. 295-322.

[13] VATHYLAKIS, A., CHONG, T.P., PARUCHURI, C., JOSEPH, P. F., 2016, "Acoustic and hydrodynamic analysis of the flow around an aerofoil with trailing-edge serrations", *22st AIAA/CEAS Aeroacoustics Conference.*

[14] CHASE, D.M., 1987, "The character of the turbulent wall pressure spectrum at subconvective wavenumbers and a suggested comprehensive model", *Journal of Sound and Vibration*, Vol. **112**, pp. 125-147

[15] BROOKS, T.F., MARCOLINI, M.A., POPE, D.S., 1984, "Airfoil trailing edge flow measurements and comparison with theory incorporating open wind tunnel corrections", *Proc. AIAA/NASA 9th Aeroacoustics Conference*, 1-12.

[16] WINKLER, J., TEMEL, F.Z., CAROLUS, T., 2007, "Concept, design and characterization of a small aeroacoustic wind tunnel facility with application to fan blade measurements", *Fan Noise*, pp. 1-12.

[17] GERHARD, T., 2015, "Umströmte Tragflügelsegmente: Auswirkungen des Hinterkantenausblasens auf Strömungsgrenzschicht und Schallemission", *Ph. D. thesis*, Universität Siegen.